Available online at www.sciencedirect.com
SCIENCE DIRECT
Polymer 45 (2004) 8075–8083
polymer
www.elsevier.com/locate/polymer

Computer simulation of polypropylene/organoclay nanocomposites: characterization of atomic scale structure and prediction of binding energy

Radovan Toth[a,c], Alessandro Coslanich[a], Marco Ferrone[a], Maurizio Fermeglia[a], Sabrina Pricl[a,*], Stanislav Miertus[b], Emo Chiellini[c,*]

[a]*Computer-aided Systems Laboratory, Department of Chemical Engineering, University of Trieste, Piazzale Europa 1, 34127 Trieste, Italy*
[b]*International Center for Science and High Technology, ICS-UNIDO, Area Science Park, Padriciano 99, 34012 Trieste, Italy*
[c]*Department of Chemistry and Industrial Chemistry, University of Pisa, Via Risorgimento 35, 56126 Pisa, Italy*

Received 23 July 2004; received in revised form 10 September 2004; accepted 12 September 2004
Available online 30 September 2004

Abstract

Molecular simulation techniques are used to explore and characterize the atomic scale structure, and to predict binding energies and basal spacing of polymer/clay nanocomposites based on polypropylene (PP) and maleated polypropylene (PPMA), montmorillonite (MMT), and different alkylammonium ions (quats) as surfactants. Our evidences suggest that shorter hydrocarbonic chains are more effective in producing favorable binding energies with respect to longer ones, and the substitutions of hydrogen atoms with polar groups on the quaternary ammonium salt (quat) generally results in greater interaction between quat and both polymer and clay. Under the hypothesis, that montmorillonite platelets are uniformly dispersed in a polymer matrix, the modified polypropylene yields higher interfacial strength with clay than neat polypropylene. The use of neat PP and quats with higher molecular volume offer the higher values of the basal spacing and thus, in principle, they should be more effective in the exfoliation process.

Keywords: Polypropylene/clay nanocomposites; Binding energies; Molecular simulations

1. Introduction

The subject of hybrids based on layered inorganic compounds such as clays has been studied for a considerable time, but the area is enjoying a resurgence of interest and activity as a result of the exceptional properties which can be realized from such nanocomposites [1–11]. Materials variables which can be controlled and which can have a profound influence on the nature and properties of the final nanocomposite include the type of clay, the choice of clay pre-treatment, the selection of polymer component and the way in which the polymer is incorporated into the nanocomposite. The last of these may be dictated by the available processing methods and whether the prospective user is an integrated polymer manufacturer or a specialist processor.

Common clays are naturally occurring minerals, and are thus subjected to natural variability in their constitution. Many clays are aluminosilicates, which have a sheet-like (layered) structure, and consist of silica SiO_4 tetrahedra bonded to alumina AlO_6 octahedra in a variety of ways. A 2:1 ratio of the tetrahedra to the octahedra results in smectite clays, the most common of which is montmorillonite (MMT). Other metals such as magnesium may replace the aluminum in the crystal structure. Depending on the precise chemical composition of the clay, the sheets bear a charge on the surface and edges, this charge being balanced by counter-ions, which reside in part in the inter-layer spacing of the clay. The thickness of the layers (platelets) is of the order of 1 nm, and aspect ratios are high, typically 100–1500. The clays are also characterized by their ion (e.g. cation) exchange capacities, which can vary widely. One important consequence of the charged nature of the clays is

* Corresponding authors. Tel.: +39 040 558 3750; fax: +39 040 569 823.
E-mail addresses: sabrinap@dicamp.units.it (S. Pricl), emochie@dcci.unipi.it (E. Chiellini).

0032-3861/$ - see front matter © 2004 Elsevier Ltd. All rights reserved.
doi:10.1016/j.polymer.2004.09.025

that they are generally highly hydrophilic species, and hence naturally incompatible with a wide range of polymer types. A necessary prerequisite for successful formation of polymer–clay nanocomposites is therefore alteration of the clay polarity to make the clay 'organophilic'. An organophilic clay can be produced from a normally hydrophilic clay by ion exchange with an organic cation such as an alkylammonium ion. The way in which this is done has a major effect on the formation of particular nanocomposite product, and this will be addressed further below.

Although the organic pre-treatment adds to the cost of the clay, the clays are nonetheless relatively cheap feedstocks with minimal limitation on supply. As anticipated above, montmorillonite is the most common type of clay used for nanocomposite formation; however, other types of clay can also be used depending on the precise properties required from the product. These clays include hectorites (magnesium silicates), which contain very small platelets, and synthetic clays (e.g. hydrotalcite), which can be produced in a very pure form and can carry a positive charge on the platelets, in contrast to the negative charge found in montmorillonite.

The synthetic route of choice for making a nanocomposite depends on whether the final material is required in the form of an intercalated or exfoliated hybrid. In the case of an intercalate, the organic component is inserted between the layers of the clay such that the inter-layer spacing is expanded, but the layers still bear a well-defined spatial relationship to each other. In an exfoliated structure, the layers of the clay have been completely separated and the individual layers are distributed throughout the organic matrix. A third alternative is dispersion of complete clay particles (tactoids) within the polymer matrix, but this simply represents use of the clay as a conventional filler.

In recent years, there has been extensive study of the factors which control whether a particular organo-clay hybrid can be synthesized as an intercalated or exfoliated structure. Since clay nanocomposites can produce dramatic improvements in a variety of properties, it is important to understand the factors that affect delamination of the clay. These factors include, besides the exchange capacity of the clay and the polarity of the reaction medium, the chemico-physical properties of interlayer cations (e.g. onium ions or quats). By modifying the surface polarity of the clay, onium ions allow thermodynamically favorable penetration of polymer precursors into the interlayer region. The ability of a given onium ion to assist in delamination of the clay depends both on its chemical and physical properties such as, for instance, its polarity and molecular volume [14–16]. The correct selection of modified clay is essential to ensure effective penetration of the polymer or its precursor into the interlayer spacing of the clay and results in the desired exfoliated or intercalated product. Indeed, further development of compatibilizer chemistry is undoubtedly the key to expansion of this nanocomposite technology beyond the systems where success has been achieved to date. Polymer can be incorporated either as the polymeric species itself or via the monomer, which is polymerized in situ to give the corresponding polymer–clay nanocomposite. The second of these is currently the most successful approach, although it probably limits the ultimate applicability of these systems. Polymers can be introduced by melt blending, for example extrusion, or by solution blending. Melt blending (compounding) depends on shear to help delaminate the clay and can be less effective than in situ polymerization in producing an exfoliated nanocomposite.

Both thermosets and thermoplastics have been incorporated into nanocomposites, including polypropylene (PP). In this respect, polypropylene has many advantages, such as easy processability, corrosion resistance, mechanical rigidity, low density and low cost. However, polypropylene/clay nanocomposites are relatively difficult to obtain because of the excessively hydrophobic nature of PP, which renders this macromolecule incompatible even with clays modified by surfactants bearing long alkyl chains. One of the methods to prepare organoclay nanocomposites from polypropylene is to improve its compatibility by the addition of polar monomers such as maleic anhydride [1–4,12,13].

Because of the strong role played by thermodynamics in delamination/exfoliation processes, evidently all quats cannot be equally effective in the preparation of PP clay nanocomposites. Therefore, two fundamental questions remain to be answered. For instance (a) what chemistry will best delaminate/exfoliate a clay in the polypropylene, and (b) which of these quats are most effective in providing stronger interactions and high interfacial strength between the dispersed clay platelets and the polyolefine?

In this work we are trying to resolve second question since the first problem involves mass transport and polymer diffusion, whose simulations are impractical at atomistic level. The basic machinery of the procedure [15,16] consists in building a molecular model comprising polypropylene (or maleated polypropylene), a given quat and MMT platelet, refining and equilibrate it by molecular mechanics/molecular dynamics (MM/MD), and calculating the binding energies as guidelines for screening among different quats to make polypropylene/nanocomposites characterized by strong interface between dispersed clay platelets and the polyolefine matrix.

2. Computational details

A simplified model assuming all montmorillonite platelets to be at low volume concentration and fully dispersed in the polymer matrix in such a way that they do not interact consists of polymer molecules interacting with quats and exposed silicate surface on one side of a MMT clay platelet [14–16].

The chemical structure of MMT is derived from the mineral pyrophyllite by random substitution of Al by Mg ions. The principal building element of this mineral are 2-D

arrays of aluminum-oxygen-hydroxyl octahedra sandwiched between two 2-D arrays of silicon -oxygen tetrahedra, forming a three-layered platelet. Thus, starting from relevant crystallographic coordinates [17] we built the unit cell of pyrophyllite crystal using the Crystal Builder modulus of the Cerius^2 molecular modeling package (v. 4.2, Accelrys, San Diego, CA, USA). To obtain the corresponding crystal structure of MMT, some aluminum ions were substituted by magnesium ions. The resulting lattice is monoclinic, with space group *C2/m*, and characterized by the following lattice parameters: $a=5.20$ Å, $b=9.20$ Å, $c=10.13$ Å and $\alpha=90°$, $\beta=99°$, $\gamma=90°$. The partial coordinates for MMT are listed in Table 1.

Several ammonium salts were considered as potential surfactants in this study, and are reported in Table 2. TMSt quat has been selected as benchmark since it has been shown experimentally to be moderately effective in enhancing intercalation of polypropylene, leading to exfoliation [4]. Due to the slightly more polar nature of maleated polypropylene with respect to neat polypropylene, in principle quats bearing polar substituents could be expected to exhibit enhanced compatibility with this polymer. Accordingly, to verify this hypothesis, some –OH, or –COOH groups have been introduced in the terminal positions of the quat structure.

The model structures of all quats were generated using the 3D sketcher tool of Cerius^2. All molecules were subjected to an initial energy minimization using the Universal force field [18] (UFF), the convergence criterion being set to 10^{-4} kcal/(mol Å). The choice of the UFF resulted from a compromise between good accuracy and availability of force field parameters for all atom types present in the molecular model. Probably the most crucial and important aspect of these calculations is the method selected for sampling the relevant configurational phase space. Accordingly, the conformational search was carried out using a well-validated combined molecular mechanics/molecular dynamics simulated annealing (MDSA) protocol [19,20], in which the relaxed structures were subjected to five repeated temperature cycles (from 600 to 1200 K and back) using constant volume/constant temperature (NVT) MD conditions. At the end of each annealing cycle, the structures were again energy minimized to converge below 10^{-4} kcal/(mol Å), and only those structures corresponding to the minimum energy were used for further modeling. The electrostatic charges for the geometrically optimized quat molecules were obtained by restrained electrostatic potential fitting [21], and electrostatic potentials were produced by single-point quantum mechanical calculations at the Hartree–Fock level with a 6-31 G basis set. All ab initio calculations were carried out with DMol^3 [22] as implemented in the Materials Studio modeling suite (v. 3.2, Accelrys, San Diego, CA, USA).

Table 1
Atomic coordinates for montmorillonite [17]

Atom	Partial coordinates		
	x/a	*y/b*	*z/c*
Al	0.000	0.333	0.000
K	0.500	0.000	0.500
Mg	0.000	0.000	0.000
O1	0.481	0.500	0.320
O2	0.172	0.728	0.335
O3	0.348	0.691	0.110
OH	0.419	0.000	0.105
Si	0.417	0.329	0.270

Table 2
Chemical formulas, abbreviations, and names of the quats

Chemical formula	Acronym	Name
$(H_3C)_3N(C_6H_{13})$	TMH	Trimethylhexyl quat
$(H_3C)_3N(C_{12}H_{25})$	TMDd	Trimethyldodecanyl quat
$(H_3C)_3N(C_{18}H_{37})$	TMSt	Trimethylstearyl quat
$(H_3C)\ N(C_{18}H_{37})(C_2H_4OH)_2$	MStDEO	Methylstearyldiethyle-neoxid quat
$(H_3C)_3N(CH_2)_6COOH$	TMoAE	Trimethylomega-aminoe-nanthic quat
$(H_3C)_3N(CH_2)_{11}COOH$	TMoAL	Trimethylomega-amino-lauric quat
$(H_3C)_2N(C_{18}H_{37})_2$	DMDSt	Dimethyldistearyl quat

The generation of accurate model amorphous structures for polypropylene and maleated polypropylene was conducted as follows [15,16]. First, the constitutive repeating unit (CRU) was built and its geometry optimized by energy minimization again using Universal force field. Hence, the CRU was polymerized to a conventional degree of polymerization (DP) equal to 15. Although this chain may be too short to capture the genuine response of a long polypropylene molecule, in the case of polystyrene (PS) it has been verified that a polymer with the same DP is longer than average persistence length of PS in polymer clay nanocomposites [23]. Explicit hydrogens were used in all model systems. The Rotational Isomeric State (RIS) algorithm [24,25] at $T=600$ K was used to create the initial polymer conformation. The structure was then relaxed to minimize energy and avoid atoms overlaps using the conjugate—gradient method. Such a straightforward molecular mechanics scheme is likely to trap the simulated system in metastable local high-energy minimum. To prevent the system from such entrapments, the relaxed structure was subjected to the same MDSA protocol applied to model the quats. At the end of each annealing cycle, the structure was again relaxed via force field, using a rms force <0.1 kcal/(mol Å).

After each component was modeled (MMT platelet, quat and PP or maleated PP), the overall system was built. The bond between the quaternary nitrogen and the methylene group of each quat was oriented perpendicularly to the *xy* plane of the mineral, and the same N atom was positioned just above the corresponding magnesium ion, but in such a way that dispersive term of the van der Waals forces were favored over the repulsive one [14–16].

To generate a proper surface, the lattice constant c of the MMT cell with five quat molecules on one side was extended to 125–150 Å depending on the length of the quats and polymer molecules. The closest distance of a part of the polymer to the quat was around 5 Å. According to previous work [14–16], this ensures that polymer chain is attracted to the quat—MMT surface by favorable nonbonded interactions, but is far away enough, so that its initial conformation hardly affects the equilibrium states of the system. Further, $c = 125$–150 Å assures that polymer molecule does not interact with K^+ surface of the nearest neighbor platelet. In other words, even if our model is 3-D periodic, there are no interactions between the periodic images in the z-direction, creating a pseudo 2 D periodic system [31].

Isothermal–isochoric (NVT) molecular dynamics experiments were run at 600 K. A high temperature was chosen so that system could quickly be equilibrated. During the simulations the positions of the MMT and K^+ atoms were fixed, but the polymer molecule and the quats were allowed to move accordingly. Each MD run was started by assigning initial velocity for atoms according to Boltzmann distribution at $2\times$T. It consisted in an equilibration phase of 50 ps, during which system equilibration was monitored by recording the instantaneous values of total, potential and nonbonded energy, and data collection phase, which was extended up to 300 ps.

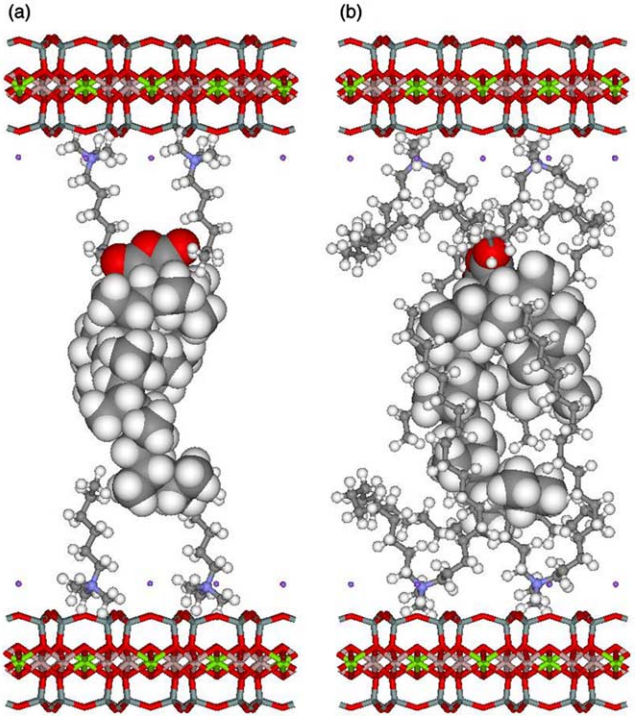

Fig. 1. Three component model used for basal spacing simulations, consisting of two layers of MMT with K^+ cations (stick model), four molecules of trimethylammonium quat (a) or dimethylstearylammonium quat (b) (stick and ball model), and one molecule of maleated polypropylene (ball model).

The total potential energy of a ternary system composed, for example, by poly(propylene), montmorillonite and a quat, $E_{(PP/MMT/quat)}$, may be written as [14–16]:

$$E_{(PP/MMT/quat)} = E_{PP} + E_{MMT} + E_{quat} + E_{PP/MMT} + E_{PP/quat} + E_{MMT/quat} \quad (1)$$

where the first three terms represent the energy of polypropylene, MMT and quat (consisting of both valence and nonbonded energy), and the last three terms are the interaction energies between each of two component pairs (made up of nonbonded terms only). By definition, the binding energy is the negative of the interaction energy.

To calculate the binding energy $E_{bind}(PP/MMT)$, for example, we first created a polypropylene–montmorillonite system deleting the quat molecules from an energy minimized conformation and calculated the potential energy of the system $E(PP/MMT)$ without further minimization. Next, we deleted the MMT platelet and K^+ ions leaving a polypropylene molecule alone, and thus calculated the energy of the PP molecule, E_{PP}. Similarly, we deleted a polypropylene molecule from the polypropylene–montmorillonite system and calculated E_{MMT}. Then, the binding energy $E_{bind}(PP/MMT)$ can be calculated from the following equation:

$$E_{bind}(PP/MMT) = E_{PP} + E_{MMT} - E(PP/MMT) \quad (2)$$

Similarly, the binding energies $E_{bind}(PP/quat)$ and $E_{bind}(MMT/quat)$ can be computed as follows:

$$E_{bind}(PP/quat) = E_{PP} + E_{quat} - E(PP/quat) \quad (3)$$

$$E_{bind}(MMT/quat) = E_{MMT} + E_{quat} - E(MMT/quat) \quad (4)$$

The estimation of the molecular surface areas and volumes was performed via the Connolly dot algorithm [26–28], corrected to account for quantum effects using the method proposed by Rellick and Becktel [29]. In this way, no assumption was made about the value of the radii of individual atoms [30].

As another piece of information on these systems, we performed further molecular dynamics simulations for the determination of the basal spacing of nanocomposite resulting from the assembly of different polymers (maleated and pristine PP), and different quats. Accordingly, we have built a three component model consists of two layers of montmorillonite, several quat molecules and a polymer chain. Fig. 1 shows an example of the molecular model for the smallest and the largest quat considered in this work, respectively. The c values in the initial model of montmorillonite crystal supercells were prolonged according to a bi-layer arrangement of the quaternary ammonium salts. After the system energy relaxation process, carried out by using Universal force field, isothermal–isobaric (NPT) MD experiments were run in a Cerius^2 modeling

enviroment at 600 K. Simulations were run for a total time of 250 ps (i.e. 250,000 steps with integration time step of 1 fs). The Ewald summation method was used to handle long range nonbonded interaction. During each MD, both montmorillonite layers were treated as rigid bodies by fixing all cell dimensions except for *c*, and all atoms in the interlayer space including K^+ cations were allow to move without any constraint.

3. Results and discussion

In order to illustrate the molecular conformations near the clay surface, we report three snapshots (see Fig. 2) taken from a molecular dynamics simulation at $T=600$ K of the system made up by a maleated polypropylene and MMT platelet exchanged with TmoAL quat. The kinetic energy fluctuates around 850 kcal/mol throughout the data

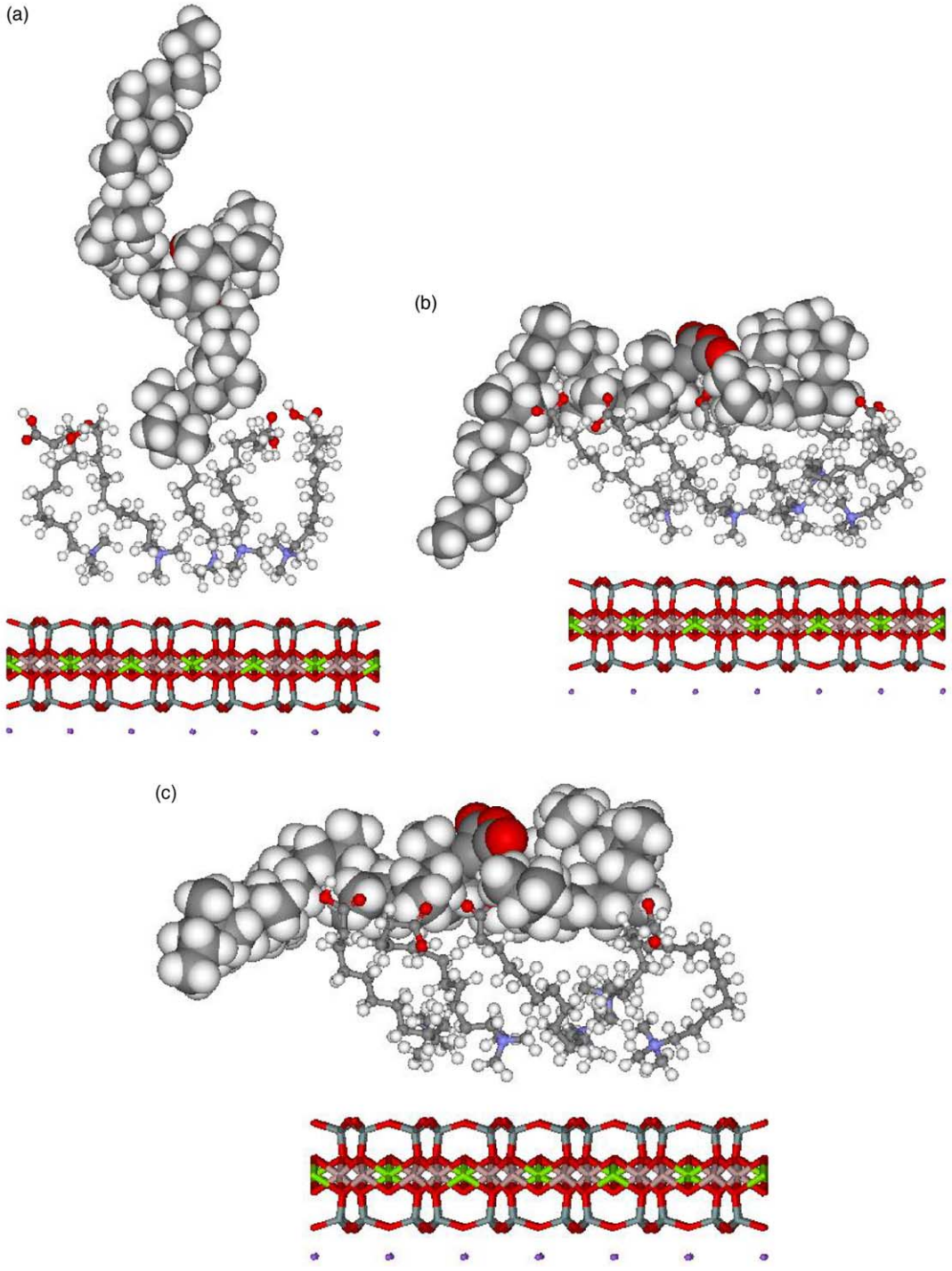

Fig. 2. Three frames extracted from MD trajectory at $T=600$ K of a system comprising a maleated PP (ball model) and a MMT platelet (stick model) exchanged with TMoAL quat (stick and ball model):(a) 0 ps; (b) 50 ps; (c) 100 ps.

harvesting phase, confirming good temperature control (Fig. 3), while the potential energy rapidly decreases and remains constant around 300 kcal/mol, by virtue of the strongly favorable nonbonded interactions (see Fig. 3). The van der Waals component of the potential energy decreases as the polymer becomes close to the MMT surface, and the Coulombic term first decreases rapidly and then stabilizes to a constant value.

As the simulation progresses, the surfactant chains flatten onto the clay, covering almost the entire surface, so the polymer can occupy only a small portion of it, if any. In other words, the polymer molecules collapse onto the quats themselves rather than directly on the clay surface. As the quats shield the interactions between the clay and the polymer, the larger the quat the larger the shielding effect. The adsorption of the hydrocarbon chains on the MMT layer of the clay surface finds its origin in the resulting, favorable electrostatic interactions. Quat molecule has a neat positive charge [14–16], which is not restricted on the nitrogen atom, but delocalized over the entire molecule. As long as they are separated by more than the sum of their van der Waals radii, interactions between the MMT oxygen and the surfactant carbon atoms are always attractive, being mainly electrostatic and secondarily van der Waals. If we now consider the shape of the quat molecules, and the fact that the average value of their surface area (SA) is rather large, it is easy to understand that all quats cannot lie flat onto the MMT surface. Some are up against the clay surface, others are next to the other quat molecules. Consequently, they form a multicarbon layer. These situations are illustrated in Fig. 4, where the side and top views of the smallest and the largest quat considered in this work, respectively, are reported for comparison. From these figures we can infer that, in the second case, the quat layer is considerably thicker that in the former one.

From the equilibrium conformation of the corresponding system we first calculated self and interaction energies, followed by the binding energies between all the components. Tables 3 and 4 summarize these results. Three different behaviors can be highlighted. The binding energy between MMT and polymer decreases in almost linear fashion with increasing quat molecular volume. Therefore, in principle, smaller quats should provide more efficient interfaces than bigger ones, as displayed in Fig. 5. The binding energy between quat and polymer slightly increases with increasing quat molecular volume, whereas the term E_{bind}(MMT/quat) has an interesting behavior. On the one side, the binding energy is affected by length of the quat tail (ultimately by the volume), and we can observe a decreasing trend of the binding energy with increasing numbers of atoms in quat tail. This is sensibly due to the prevalence of the unfavorable interactions between individual quat tails and weaker electrostatic interactions between MMT and quat due to tail offs. On the other hand, E_{bind}(MMT/quat) is also influenced by the introduction of polar groups in the quats: indeed, the presence of these groups results in an increase of the binding energy between clay and quats, as we can see when we compare quats almost with same molecular volume, but different number of polar groups (consider, for instance, TMH and TMoAE).

Since quats shield interactions between polymer and clay, the combination of pristine clay with maleated polypropylene produces the highest binding energy of all, as confirmed by our calculations (see Tables 3 and 4). Thus, nanocomposites produced from untreated clays should be the toughest. On the other hand, there is a problem to

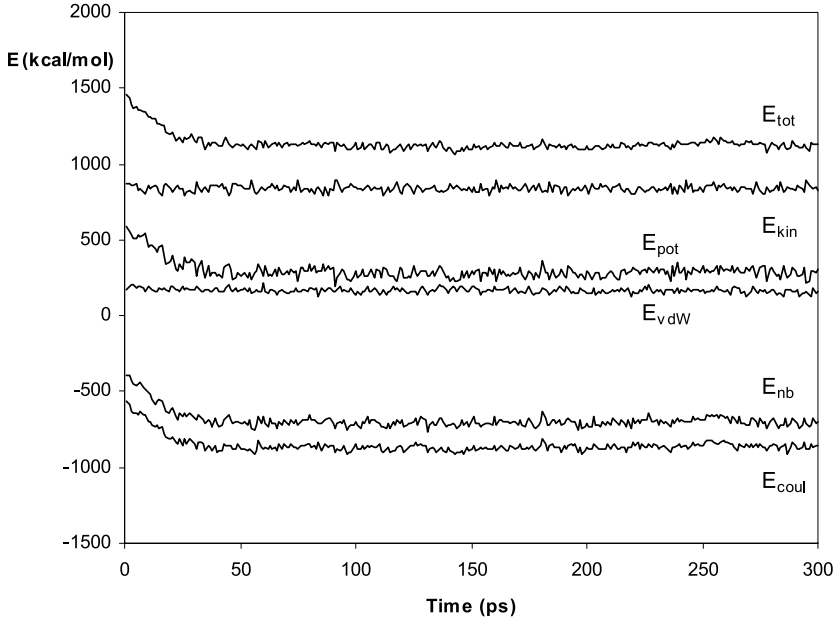

Fig. 3. Profiles of the energy components for the simulation shown in Fig. 2. E_{tot}: total energy, E_{kin}: kinetic energy, E_{pot}: potential energy, E_{vdW}: van der Waals energy, E_{nb}: total nonbonded energy, and E_{coul}: coulombic energy.

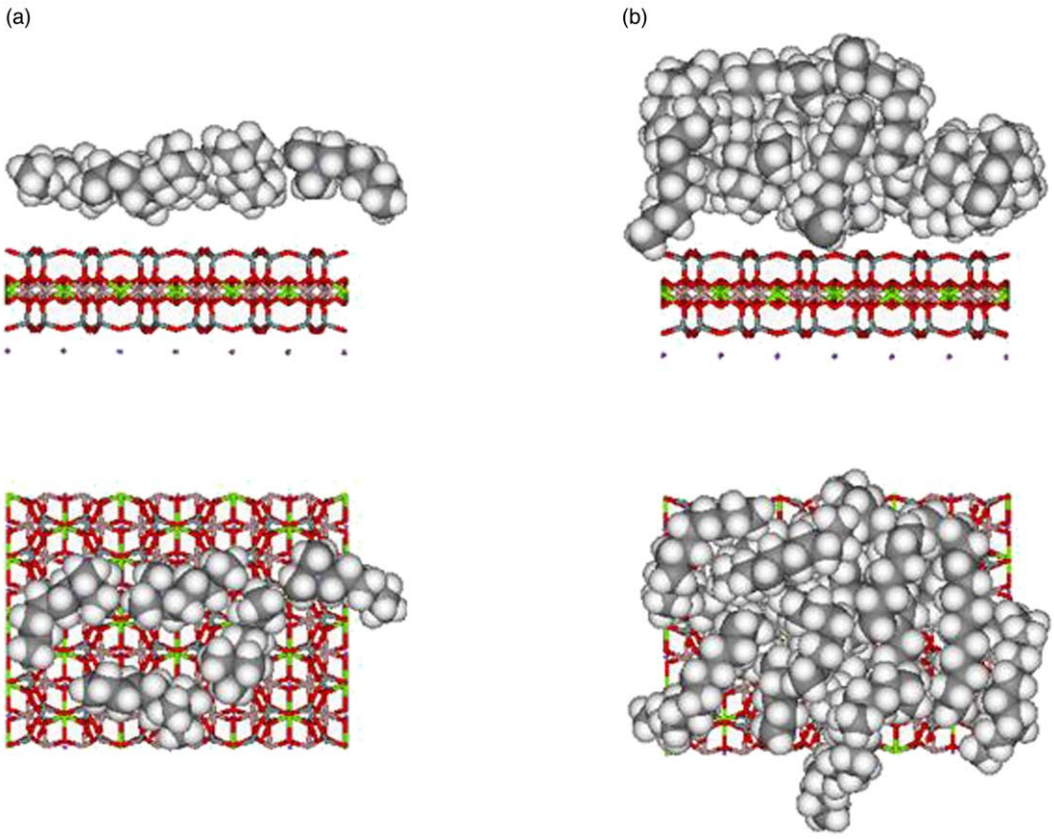

Fig. 4. Top and side view of a clay with (a) TMH quat and (b) DMDSt quat conformation after equilibration. MMT layer (stick model), quats (ball model).

intercalate polymer within pristine montmorillonite platelets due to hydrophilic surface of the MMT platelet. Accordingly, another question arises at this point: which quat will be most effective in the intercalation of the polymer between MMT platelets, and will provide the highest interfacial strength between clay and polymer?

We can observe that maleated polypropylene (PPMA) yields higher binding energy than neat polypropylene, due to polar group on the polypropylene backbone (see Tables 3 and 4). It is not clear, however, whether the binding energy between the clay and polymer alone is sufficient to determine the fracture toughness or the breaking strength. Since the quat molecules adsorb onto the clay surface, it may be more reasonable to use the sum of E_{bind}(PPMA/MMT) and E_{bind}(PPMA/quat) as a better measure of surface energy contribution. Fig. 6 displays the dependence of this sum on quat volume. Since the increase in E_{bind}(PPMA/quat) is smoother that decrease of E_{bind}(PPMA/MMT) with the same quantity, the sum still decreases with increasing quat molecular volume.

To limit computational time to reasonable limits, we considered only a couple of three-component systems for further modeling, devoted to the determination of the corresponding basal spacing. The components were chosen on the basis of the corresponding energetic calculations; accordingly, only the surfactant molecules that resulted in

Table 3
Binding energies calculated from simulation according to Eqs. (1)–(3) using maleated PP, and molecular areas and volumes of quats

Chemical formula	$E_{bind}^{PPMA/MMT}$ (kcal/mol)	$E_{bind}^{PPMA/quat}$ (kcal/mol)	$E_{bind}^{MMT/quat}$ (kcal/mol)	SA (Å^2)	V (Å^3)
Pristine	124				
$(H_3C)_3N(C_6H_{13})$	115.1	47.0	1325	239	179
$(H_3C)_3N(CH_2)_{6-}$ COOH	111.6	49.6	1566	275	207
$(H_3C)_3N(C_{12}H_{25})$	87.6	63.1	1247	370	281
$(H_3C)_3N(CH_2)_{11-}$ COOH	82.5	74.5	1320	381	292
$(H_3C)_3N(C_{18}H_{37})$	45.3	83.1	1109	497	383
$(H_3C)N(C_{18}H_{37})(C_{2-}$ $H_4OH)_2$	33.6	85.1	1267	560	433
$(H_3C)_2N(C_{18}H_{37})_2$	13.8	103.0	1096	752	665

Table 4
Binding energies calculated from simulation according to Eqs. (1)–(3) using neat PP, and molecular areas and volumes of quats

Chemical formula	$E_{bind}^{PP/MMT}$ (kcal/mol)	$E_{bind}^{PP/quat}$ (kcal/mol)	$E_{bind}^{MMT/quat}$ (kcal/mol)	SA (Å^2)	V (Å^3)
Pristine	98.0				
$(H_3C)_3N(C_6H_{13})$	117.0	58.4	1471	239	179
$(H_3C)_3N(C_{12}H_{25})$	84.9	52.0	1247	370	281
$(H_3C)_3N(C_{18}H_{37})$	27.3	93.1	1155	497	383
$(H_3C)_2N(C_{18}H_{37})_2$	15.8	99.1	1105	752	665

the highest and the lowest value of the binding energy between polymer and MMT, respectively, were selected. Table 5 shows the values of basal spacing of models with relevant compositions after 250 ps of NPT molecular dynamics simulation. From these values we can see that the system containing the quat molecule yielding the best binding energy between the polymer matrix and the montmorillonite platelet (see Tables 3 and 4) is characterized by the smallest basal spacing. On the contrary, the alternative system containing the surfactant molecule yielding the lowest binding energy value presents the highest value of the distance between the two MMT layers. The use of neat polypropylene is reflected in a smaller increase of the basal spacing, which is makes sense to ascribe to more radiating chain of neat PP with respect to maleated PP due to no presence of polar group in its backbone.

From a global interpretation of all these molecular dynamics simulation results we can conclude that, on the one hand, quats with smaller volume are more effective for clay modification as they improve the thermodynamics of the system by increasing the binding energy, while on the other hand quats with longer tails are more effective for intercalation and exfoliation processes, as they lead to higher basal spacing. Alike, for a given surfactant molecule, the use of maleated PP in the preparation of polypropylene organoclay nanocomposites results in a system with the most favorable interaction energy but with a lower basal spacing. Although no experimental data on poly(propylene) and/or PPMA-based nanocomposites are available to date, the proposed results can be considered with confidence, as the predictions obtained from same computational procedure, applied to nylon-6/MMT nanocomposites, have been recently experimentally validated by Fornes et al. [32].

Table 5
The basal spacing values of the three component models after 250 ps of NPT molecular dynamics simulations as a function of quat and polymer used

Quat	Spacing (Å)	
	PPMA	PP
$(H_3C)_3N(C_6H_{13})$	31.19	35.02
$(H_3C)_3N(C_{18}H_{37})$	36.20	38.60
$(H_3C)_2N(C_{18}H_{37})_2$	40.02	41.12

4. Conclusions

In this work, we used molecular simulation techniques to explore and characterize the atomic scale structure, and to predict binding energies and basal spacing of polymer/clay nanocomposites based on polypropylene and maleated polypropylene, montmorillonite (MMT), and different alkylammonium ions as surfactants.

The major findings of this study can by summarized as

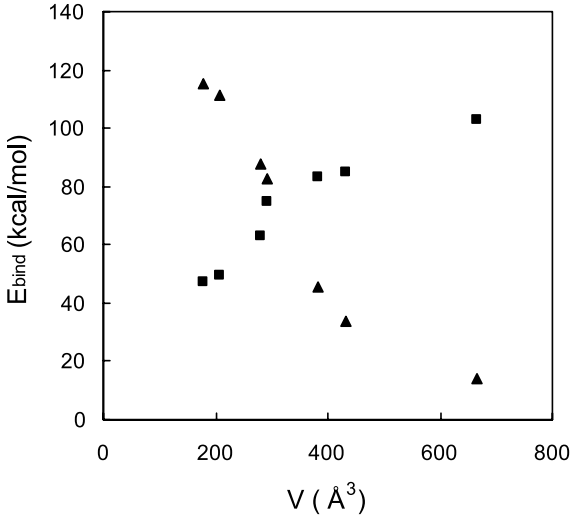

Fig. 5. Predicted binding energy versus quat volume. Squares: E_{bind}(PPMA/quat); triangles: E_{bind}(PPMA/MMT).

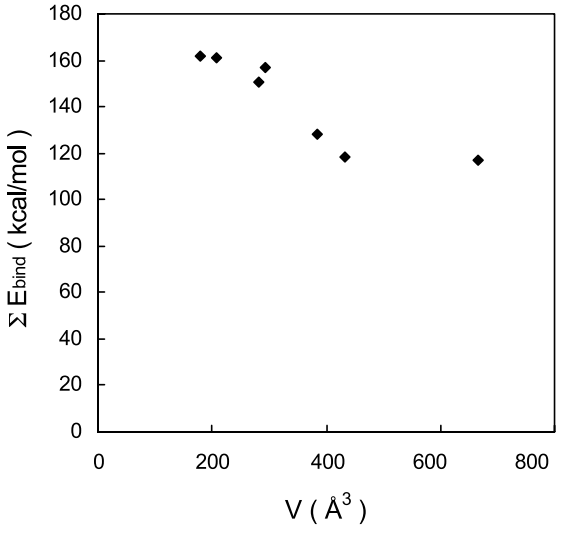

Fig. 6. Sum of E_{bind}(PPMA/MMT) and E_{bind}(PPMA/quat).

follows. The binding energy between clay and polymer decreases with increasing molecular volume of the quaternary ammonium salt used as surfactant. On the other hand, the binding energy between the polymer and quat increases with increasing molecular volume of the quat, which is reasonable. The binding energy between clay and quats is mainly affected by presence of the polar group in a quat, which reflects in an increase of E_{bind}(MMT/quat), and secondarily by quat volume. When only the quat volume parameter is considered, we can observe a decreasing trend of the E_{bind}(MMT/quat) with increasing volume of the quat. Shorter hydrocarbonic chains are more effective in producing favorable binding energies with respect to longer ones, and the substitutions of hydrogen atoms with polar groups on the quaternary ammonium salt generally results in greater interaction between quat and both polymer and clay. Under the hypothesis that montmorillonite platelets are uniformly dispersed in a polymer matrix, the modified polypropylene yields higher interfacial strength with clay than neat polypropylene. The use of neat PP and quats with higher volume yields the higher values of the basal spacing and thus, they should in principle be more effective in the corresponding exfoliation process.

Acknowledgements

The work described in the present paper has been performed within the framework of the EC-funded project NANOPROP G5RD-CT-2002-00834.

References

[1] Kodgire P, Kalgaonkar R, Hambir S, Bulakh N, Pog JP. J Appl Polym Sci 2001;81:1786–92.
[2] Koo MCh, Kim MJ, Choi MH, Kim SO, Chung IJ. J Appl Polym Sci 2003;88:1526–35.
[3] Li J, Zhou Ch, Gang W. Polym Test 2003;22:217–23.
[4] Hasegawa N, Kawasumi M, Kato M, Usuki A, Okada A. J Appl Polym Sci 1998;67:87–92.
[5] Ma J, Qi Z, Hu Y. J Appl Polym Sci 2001;82:3611–7.
[6] Kato M, Usuki A, Okada A. J Appl Polym Sci 1997;66:1781–5.
[7] Liu X, Wu Q. Polymer 2001;42:10013–9.
[8] Zhang Q, Wang Y, Fu Q. J Polym Sci Part B: Polym Phys 2003;41:1–10.
[9] Hasegawa N, Okamoto H, Kawasumi M, Kato M, Tsukigase A, Usuki A. Macromol Mater Eng 2000;280–281:76–9.
[10] Marosi Gy, Anna P, Marton A, Bertalan Gy, Bota A, Toth A, Mohai M, Racz I. Polym Adv Technol 2002;13:1103–11.
[11] Cho JW, Paul DR. Polymer 2001;42:1083–94.
[12] Reichert P, Nitz H, Klinke S, Brandsch R, Thomann R, Mulhaupt R. Macromol Mater Eng 2000;275:8–17.
[13] Marchant D, Jayaraman K. Ind Eng Chem Res 2002;41:6402–8.
[14] Tanaka G, Goettler LA. Polymer 2002;43:541–53.
[15] Fermeglia M, Ferrone M, Pricl S. Fluid Phase Equilib 2003;212:315–29.
[16] Fermeglia M, Ferrone M, Pricl S. Mol Simulation 2004;30:289–300.
[17] Tsipursky SI, Drite VA. Clay Miner 1984;19:177–93.
[18] Castonguay LA, Rappe AK. J Am Chem Soc 1992;114:5832–42.
[19] Fermeglia M, Pricl S. AIChE J 1999;45:2619–27.
[20] Metullio L, Ferrone M, Coslanich A, Fuchs S, Fermeglia M, Paneni MS, Pricl S. Biomacromolecules 2004;5:1371–8.
[21] Bayly CI, Cieplak P, Cornell WD, Kollman PA. J Phys Chem 1993;97:10269–80.
[22] Delley B. J Chem Phys 1990;92:508–20.
[23] Manias E, Kuppa V. In: Vaia R, Krishnamoorti R, editors. Polymer nanocomposite. ACS Symposium Series, vol. 804. Oxford: Oxford University Press; 2002. p. 193–207. Chapter 15.
[24] Flory PJ. Principles of polymer chemistry. Ithaca: Cornell University Press; 1974.
[25] Mattice WL, Suter UW. Conformational theory of large molecules: the rotational isomeric state model in macromolecular systems. New York: Wiley; 1994.
[26] Connolly ML. J Appl Crystallogr 1983;16:548–58.
[27] Connolly ML. Science 1983;221:709–13.
[28] Connolly ML. J Am Chem Soc 1985;107:1118–24.
[29] Rellick LM, Becktel WJ. Biopolymers 1997;42:191–202.
[30] Fermeglia M, Pricl S. Fluid Phase Equilib 1999;166:21–37.
[31] Misra S, Feming III PD, Mattice WL. J Comp Aided Mater Des 1995;2:101–8.
[32] Fornes TD, Hunter DL, Paul DR. Macromolecules 2004;37:1793–8.